Supporting Information For:

Preparation and Properties of a Series of Structurally Diverse Aluminum Hydrides Supported by β-Diketiminate and *bis*(Amide) Ligands

A. E. Nako, Sarah. J. Gates, Andrew J. P. White, and Mark R. Crimmin

DFT Studies

Computational Methods: Calculations were implemented in Gaussian09 using gview (v 5.09) as an interface. DFT studies were performed using either the B3LYP, B3P86, or M06-2X functional and 6,31G+(d,p), 6,31G+(d,p)/Lanl2DZ or TZVP basis-set. Solid-state data for **2-A, 3a** and *cis*-**4b$_2$** were used as starting geometries for gas-phase calculations and all stationary points were confirmed by frequency calculations. A series of basis-sets and functionals were investigated for **2-A** and values for the Al–N bond lengths and Al–H frequencies are compared against the experimental data in Table S1 and Figure S2. Potential energy surface scans were initiated from previously optimised ground-state geometries by varying the Al–NR$_3$ vector at 0.05 Å intervals. In order to compare the energies of the isomers formed upon variation of the Al–NR$_3$ distance, independent frequency calculations were conducted on local minimum geometries **2-D** and **2-E**. A further geometry optimization was conducted on **5** + NMe$_3$ separate at > 5.0 Å.

Figure S1. Selected bond lengths for **2-A**, **2-B** and **2-C** calculated with the M06-2X functional and 6,31G+(d,p)/Lanl2DZ basis-set.

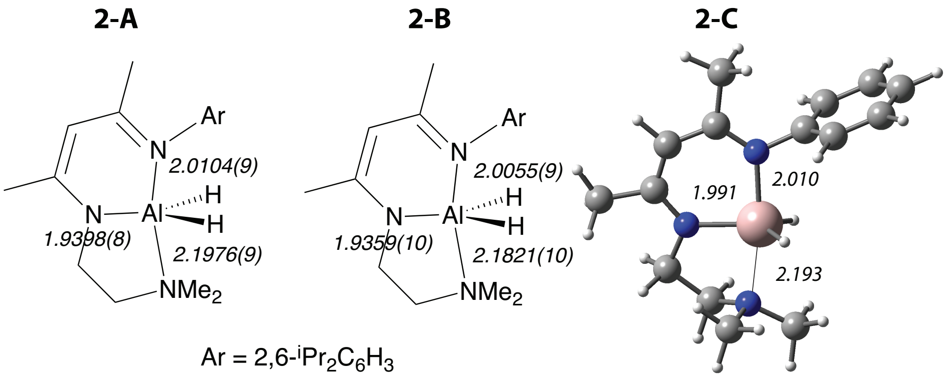

Table S1. Selected data calculated for **2-C** at various levels of theory along with the data for **2-A**. Bond lengths given in Å and stretching frequencies in cm^{-1}.

	Al–N$_{ax}$	Al–NMe$_2$	Al–N$_{eq}$	V(Al–H)
2-A	**2.0104(9)**	**2.1976(9)**	**1.9398(8)**	**1746**
B3LYP/6,31G+(d,p)	2.015	2.298	1.978	1789, 1821
B3LYP/TZVP	2.014	2.307	1.975	1785, 1814
B3LYP/6,31G+(d,p)/Lanl2DZ	2.030	2.263	1.997	1721, 1746
B3P86/6,31G+(d,p)	2.015	2.298	1.980	1797, 1829
B3P86/TZVP	2.022	2.278	1.980	1759,1726
B3P86/6,31G+(d,p)/Lanl2DZ	2.019	2.220	1.992	1716, 1739
M06-2X/6,31G+(d,p)	1.995	2.203	1.972	1800,1839
M06-2X/TZVP	1.989	2.192	1.967	1719.1744
M06-2X/6,31G+(d,p)/Lanl2DZ	2.010	2.193	1.991	1721,1745

Figure S2. Graphical representation of the systemic overestimation of the Al–NMe$_2$ bond level for various functionals and basis-sets. Values for **2-C** relative to the solid-state data for **2-A** in Å.

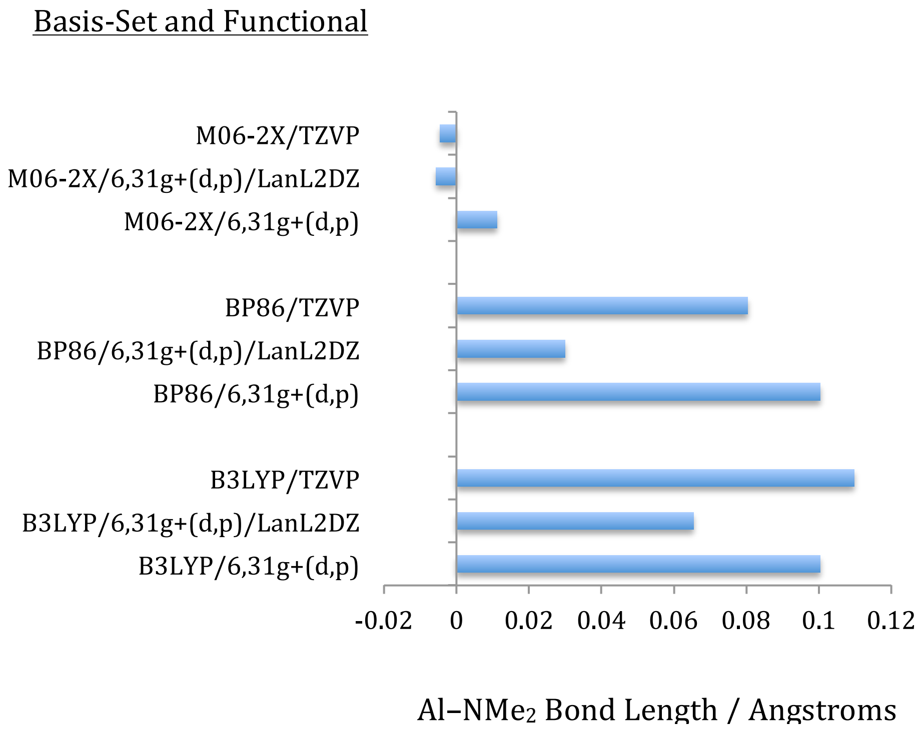

Figure S3. Scan of the potential energy surface along Al–NMe$_2$ bond of **2**. Data calculated at 0.05 Å increments.

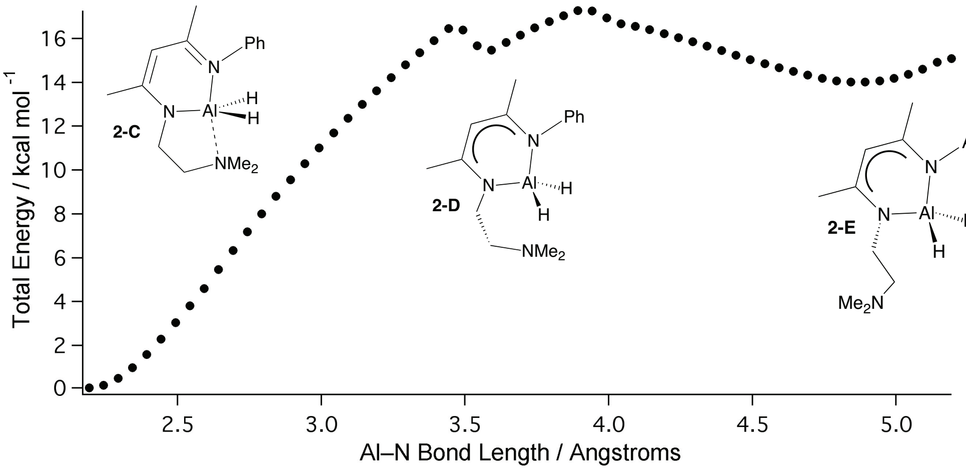

Figure S4. Scan of the potential energy surface along Al–NMe$_3$ bond of **5•NMe$_3$**. Data calculated at 0.05 Å increments.

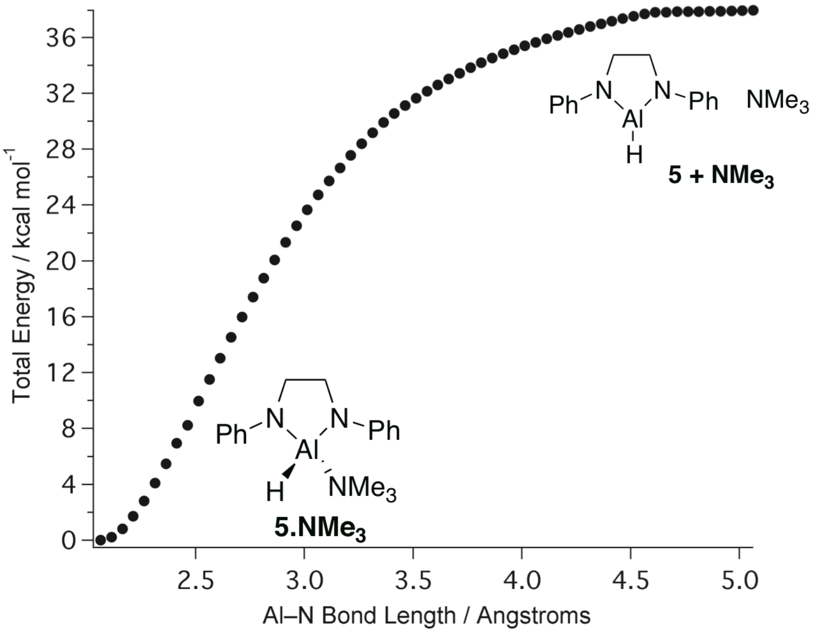

X-ray Crystallography Studies

Table S2. X-ray experiment acquisition parameters and selected data on compounds **2** and **3a**

data	2	3a
Molecular formula	$C_{21}H_{36}AlN_3$	$C_{23}H_{36}AlN_3$
Formula weight (g mol^{-1})	357.51	381.53
Crystal system	Monoclinic	Triclinic
Space group	*P*2(1)/c	*P*-1
Temperature (K)	173	173
a (Å)	18.9383(3)	8.2933(4)
b (Å)	13.30838(15)	10.1234(4)
c (Å)	18.4372(2)	14.4114(5)
α (deg)	–	103.226(3)
β (deg)	110.8573(16)	103.546(3)
γ (deg)	–	94.966(3)
V (Å^3)	4342.37(11)	1132.45(8)
Z	8[b]	2
μ (mm^{-1})	0.102	0.102
ρ (g cm^{-3})	1.094	1.119
R_1 (obs)	0.0449	0.0445
wR_2[a] (all data)	0.1326	0.1352
Unique / observed reflections	14624 / 11545	7386 / 5995
R_{int}	0.0209	0.0166

[a] $R1 = \Sigma||Fo| - |Fc||/\Sigma|Fo|$; $wR2 = \{\Sigma[w(Fo^2 - Fc^2)^2] / \Sigma[w(Fo^2)^2]\}^{1/2}$; $w^{-1} = \sigma^2(Fo^2) + (aP)^2 + bP$. [b] There are two crystallographically independent complexes.

Table S3. X-ray experiment acquisition parameters and selected data on compounds *cis*-**4b•toluene$_2$** and **6**

data	*cis*-**4b$_2$**•toluene$_2$	**6**
Molecular formula	$C_{52}H_{78}Al_2N_4$•$(C_7H_8)_2$	$C_{27}H_{31}AlN_2$
Formula weight (g mol^{-1})	997.41	410.52
Crystal system	Triclinic	Orthorhombic
Space group	*P*-1	*P*nma
Temperature (K)	173	173
a (Å)	11.5586(4)	14.3480(3)
b (Å)	11.9034(3)	18.1039(4)
c (Å)	22.9284(7)	9.2139(2)
α (deg)	91.033(2)	–
β (deg)	96.291(3)	–
γ (deg)	108.695(2)	–
V (Å^3)	2965.47(16)	2393.35(9)
Z	2	4[b]
μ (mm^{-1})	0.750	0.100
ρ (g cm^{-3})	1.117	1.139
R_1 (obs)	0.0382	0.0525
wR_2[a] (all data)	0.1032	0.1617
Unique / observed reflections	11459 / 10035	4247 / 3172
R_{int}	0.0223	0.0232

[a] $R1 = \Sigma||Fo| - |Fc||/\Sigma|Fo|$; $wR2 = \{\Sigma[w(Fo^2 - Fc^2)^2] / \Sigma[w(Fo^2)^2]\}^{1/2}$; $w^{-1} = \sigma^2(Fo^2) + (aP)^2 + bP$. [b] The complex has C_s symmetry.

The Al–H hydrogen atoms in all structures were located from Δ*F* maps and refined freely. The structure of **2** was found to contain two crystallographically independent molecules (**2-A** and **2-B**, shown in Figs. S7 and S8 respectively) that have noticeably different conformations (Fig. S9). The C(70)-based included toluene solvent molecule in the structure of **4b** was found to be disordered. Two orientations were identified, of *ca*. 77 and 23% occupancy, their geometries were optimized, the thermal parameters of adjacent atoms were restrained to be similar, and only the major occupancy non-hydrogen atoms were refined anisotropically (the remainder were refined isotropically). The structure of 6 has crystallographic Cs symmetry with Al, the Al–H hydrogen atom, C(2) and the C(12)-based phenyl ring all sitting on mirror plane. The C(4)-based 2,5-

diemthylphenyl group in the structure of 6 was found to be disordered. Two orientations were identified, of ca. 78 and 22% occupancy, their geometries were optimised, the thermal parameters of adjacent atoms were restrained to be similar, and only the major occupancy non-hydrogen atoms were refined anisotropically (the remainder were refined isotropically).

Figure S6 The structure of **2-A**, one of the two independent molecules present in the crystal of **2** (50% probability ellipsoids).

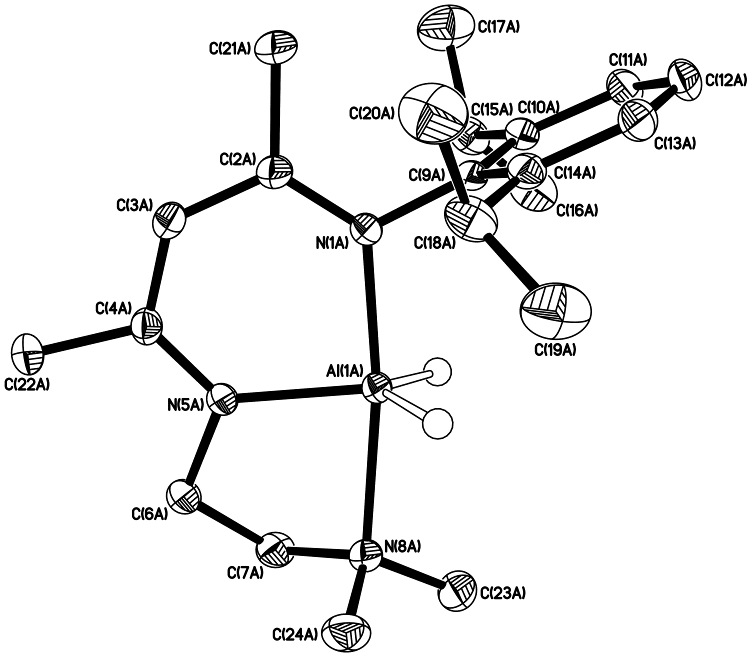

Figure S7 The structure of **2-B**, one of the two independent molecules present in the crystal of **2** (50% probability ellipsoids).

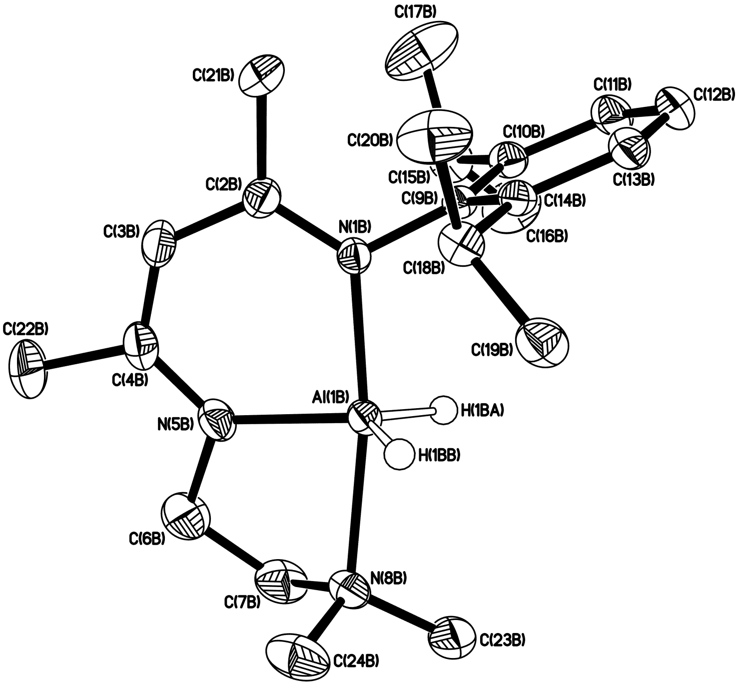

Figure S8 Overlay of the two independent molecules present in the crystal of **2**, showing the different conformations of the β-diketiminate and 2,6-di-iso-propyl moieties.

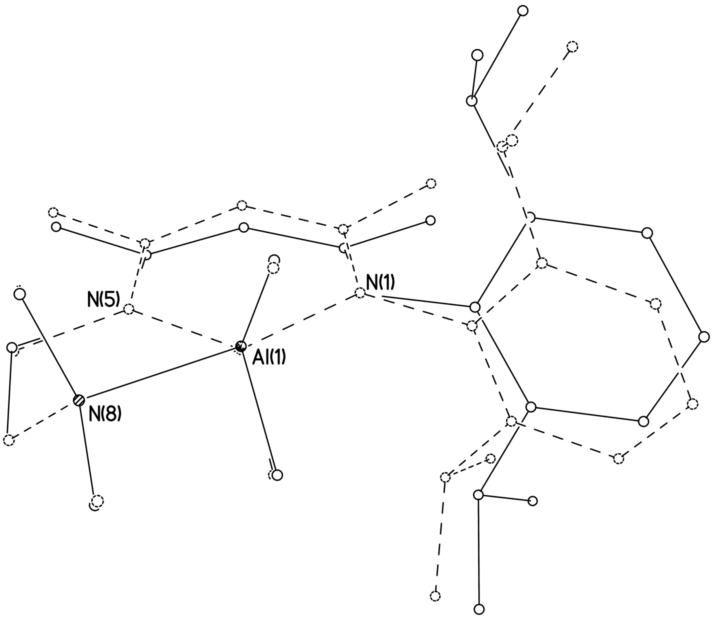

Figure S9 The crystal structure of **3a** (50% probability ellipsoids).

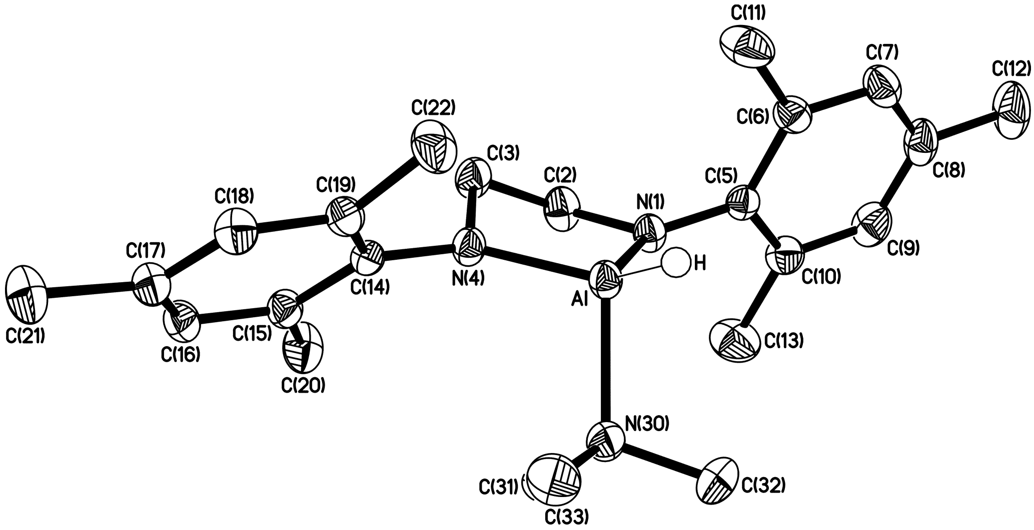

Figure S10 The crystal structure of **4b** (50% probability ellipsoids).

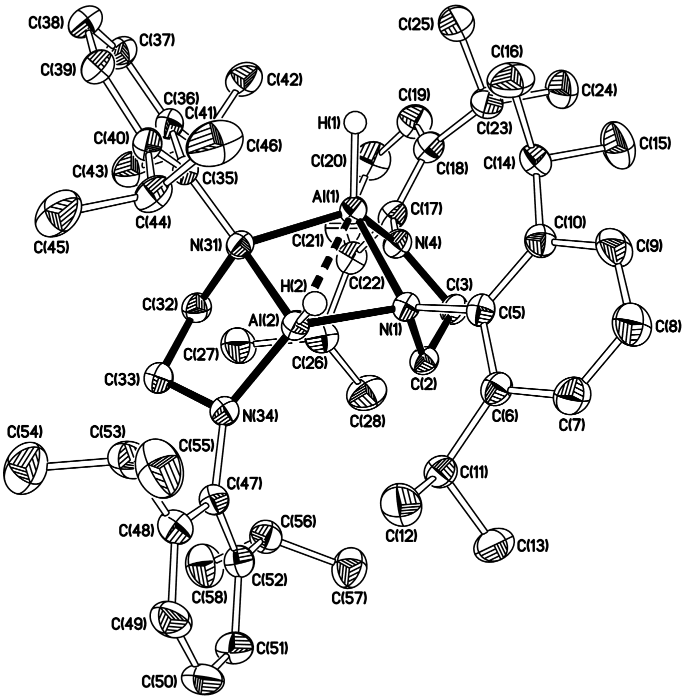

Fig. S11 The crystal structure of the C_S symmetric complex **6** (50% probability ellipsoids). Atoms labeled with an "A" after the number are related to their counterparts without the letter by the mirror plane that passes through the metal, the metal hydride, C(2) and the C(12)-based phenyl ring

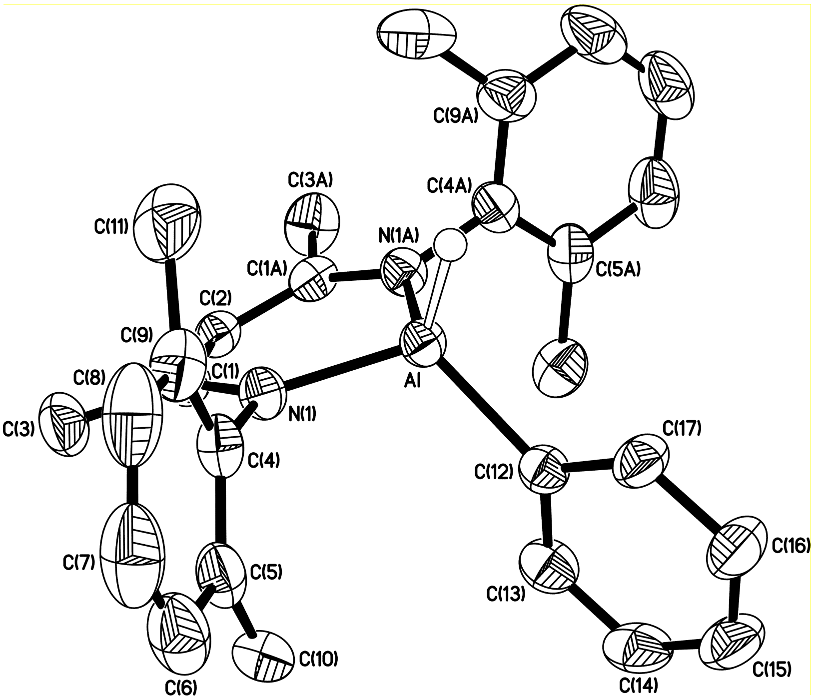

Variable Temperature NMR data on 3a and 3b

Figure S12. Variable ^{1}H NMR data from 193 – 353 K for **3a** in toluene-d^8

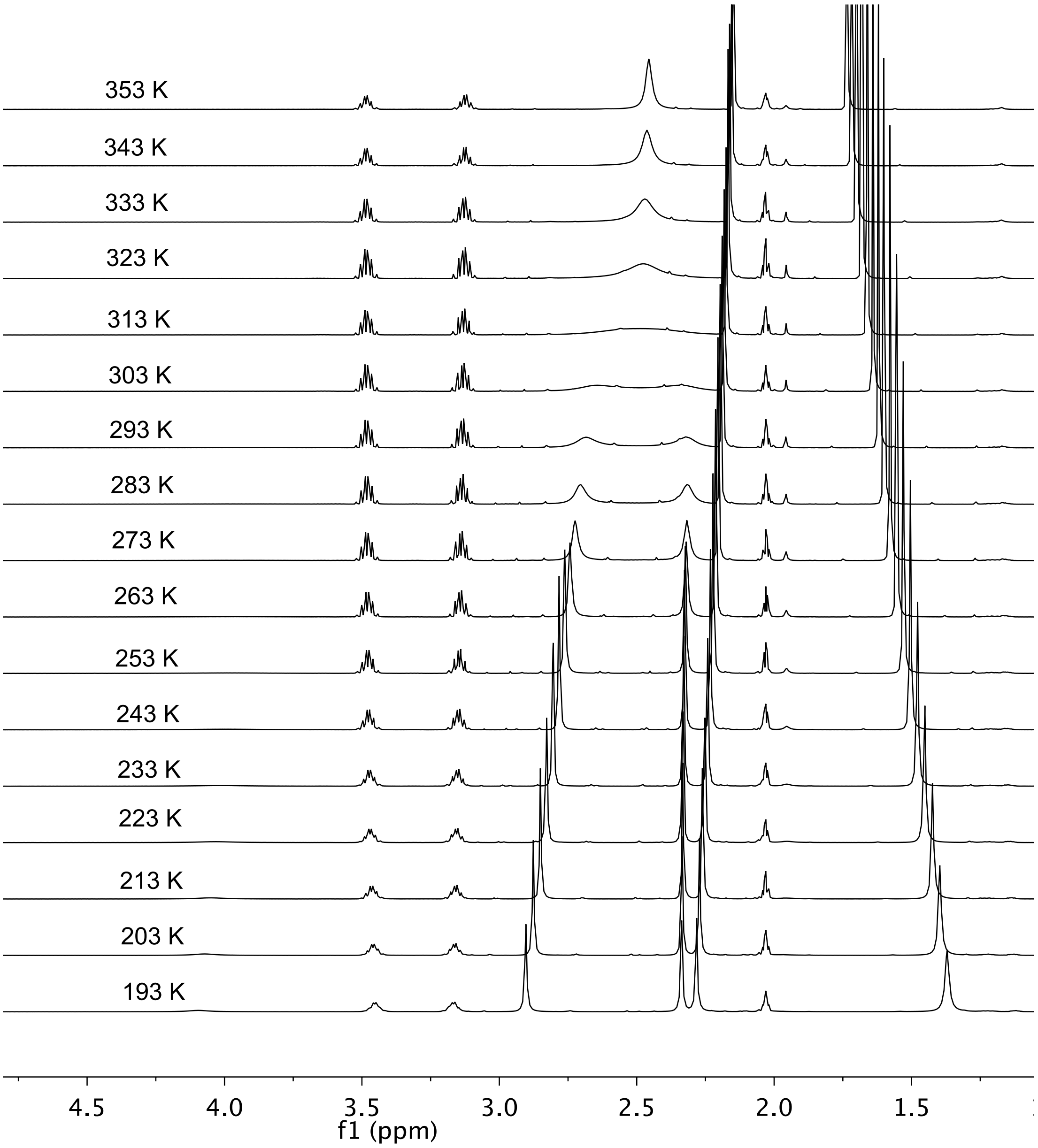

Figure S13. Variable ^{1}H NMR data from 298 – 383 K for **3b** in toluene-d^8

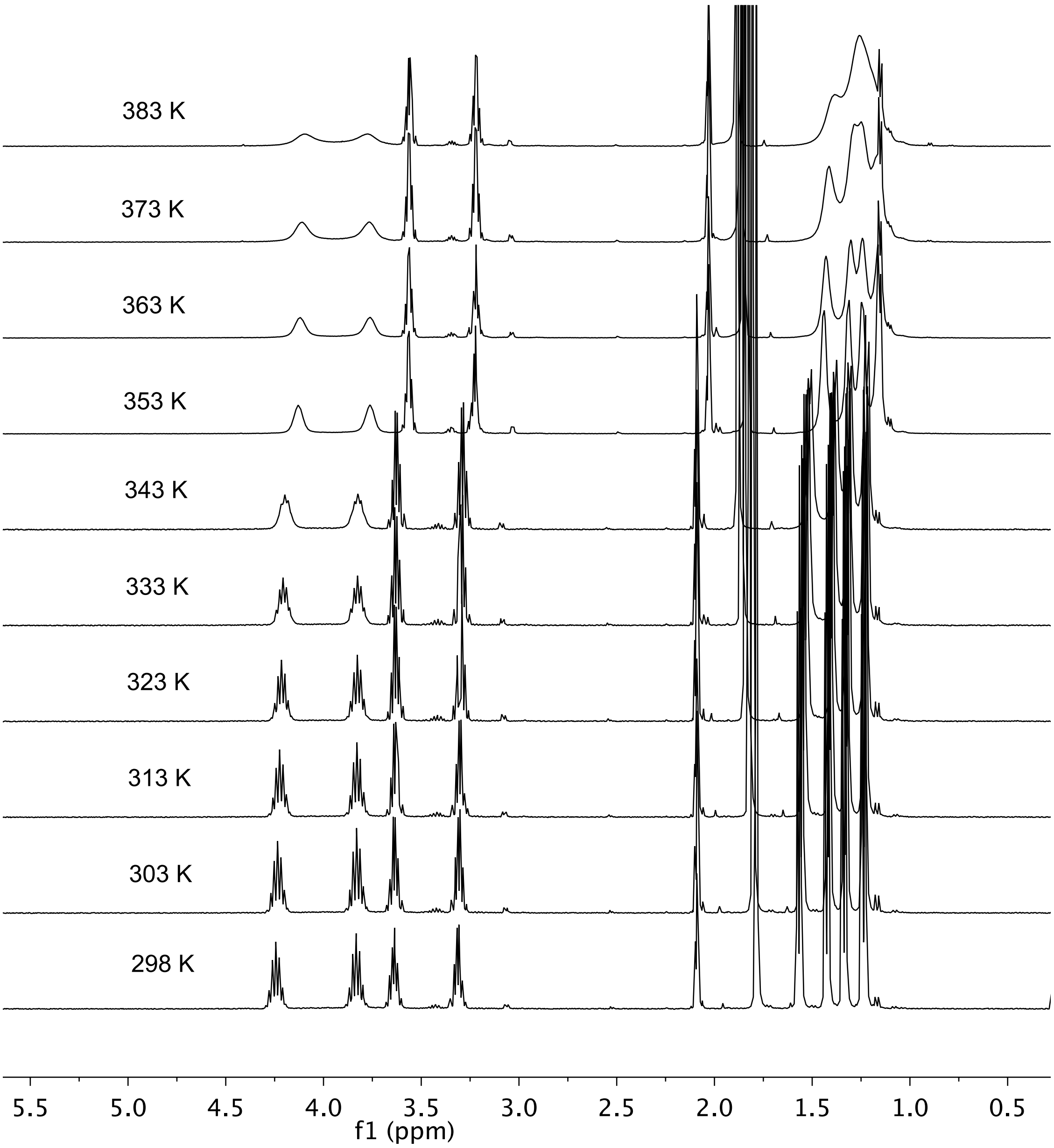

Multinuclear NMR data on Compounds 2, 3a-b, *cis*-4b$_2$ and 6

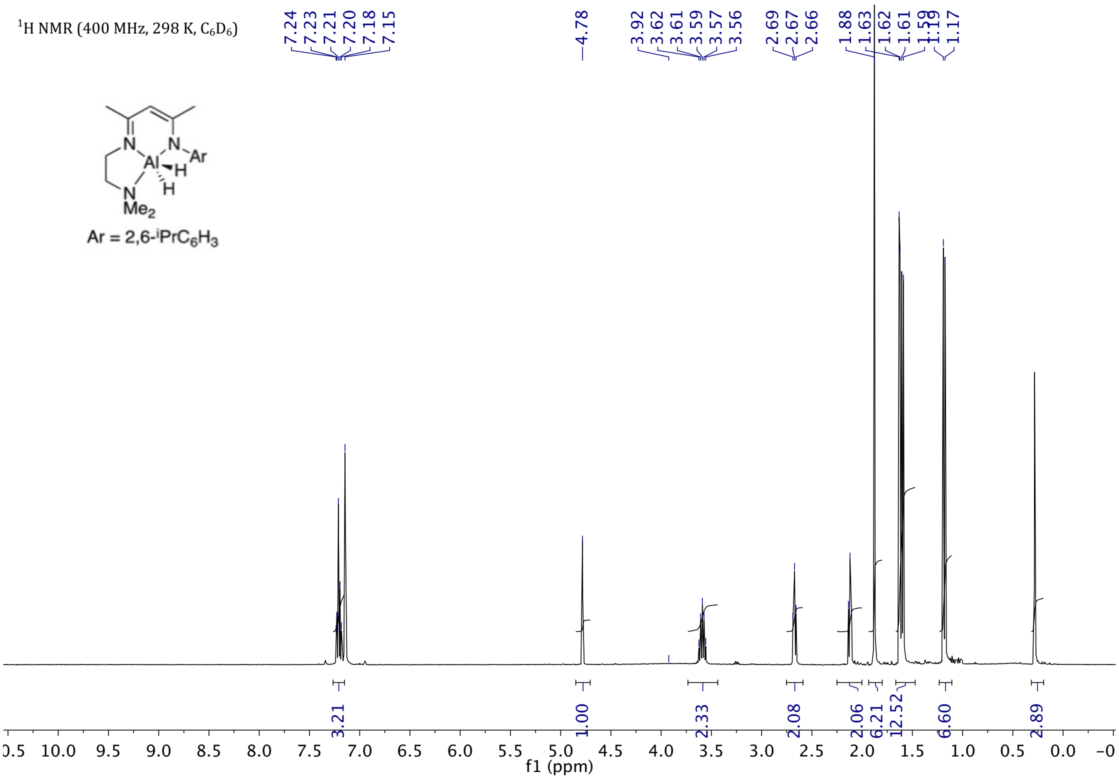

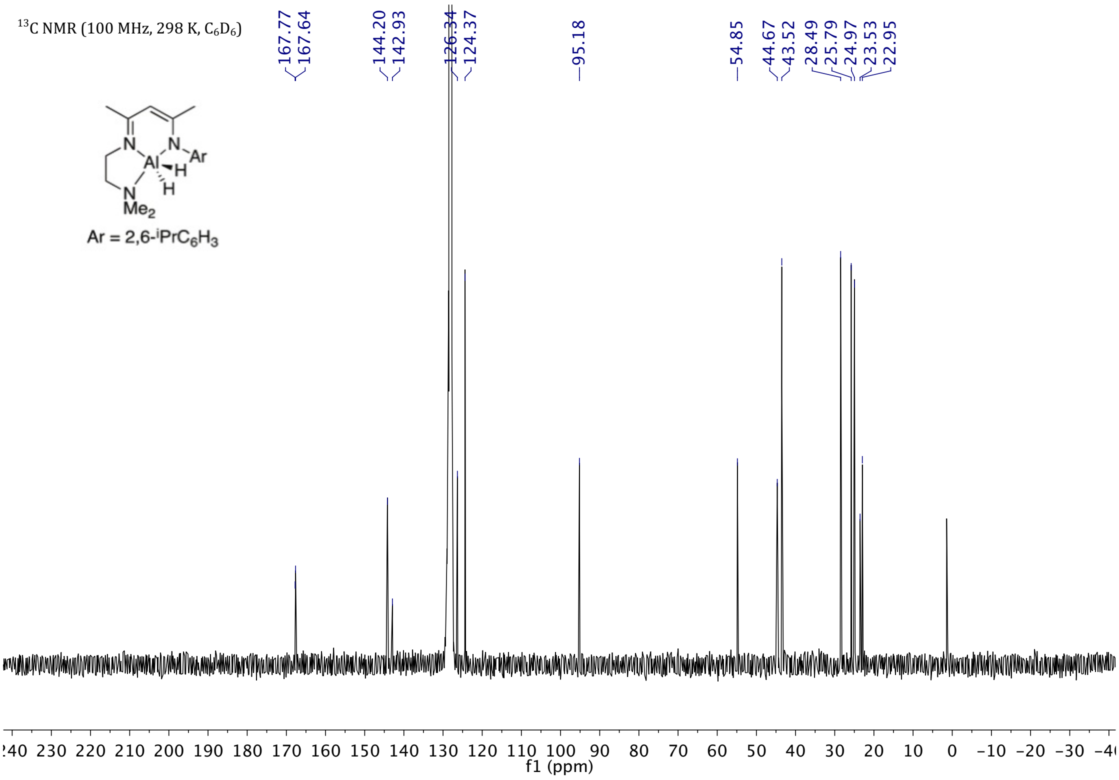

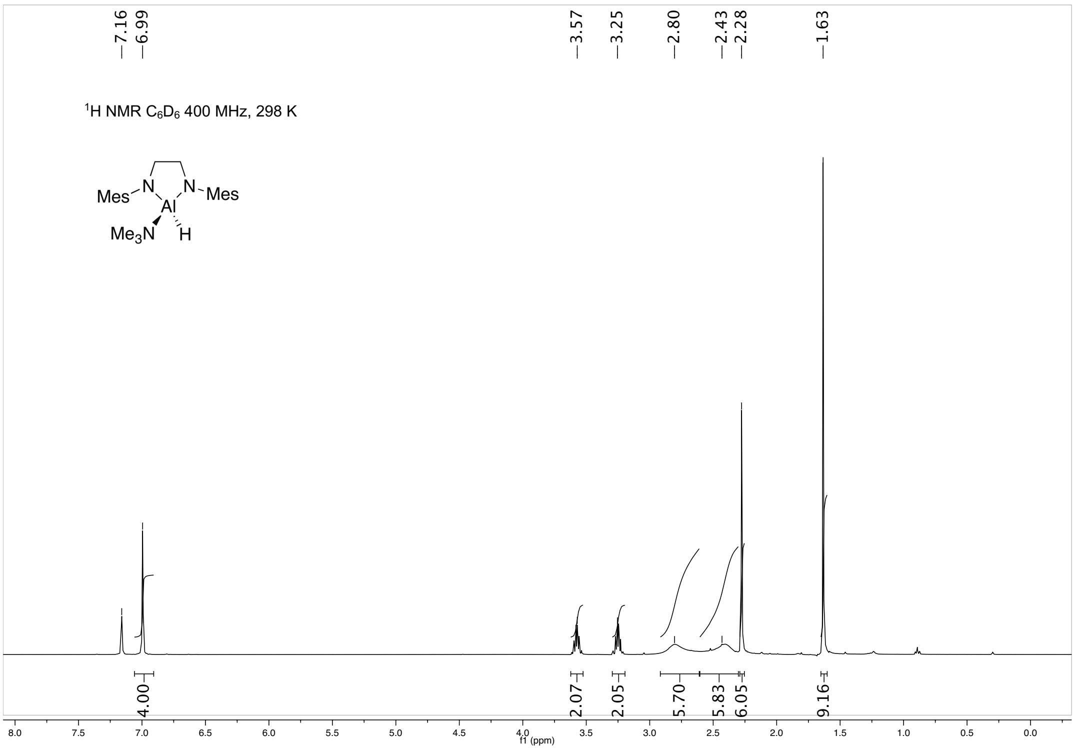
7.16
6.99
3.57
3.25
2.80
2.43
2.28
1.63
^{1}H NMR C_6D_6 400 MHz, 298 K
Mes
N
N
Mes
Al
Me_3N
H
4.00
2.07
2.05
5.70
5.83
6.05
9.16
8.0
7.5
7.0
6.5
6.0
5.5
5.0
4.5
4.0
3.5
3.0
2.5
2.0
1.5
1.0
0.5
0.0
f1 (ppm)

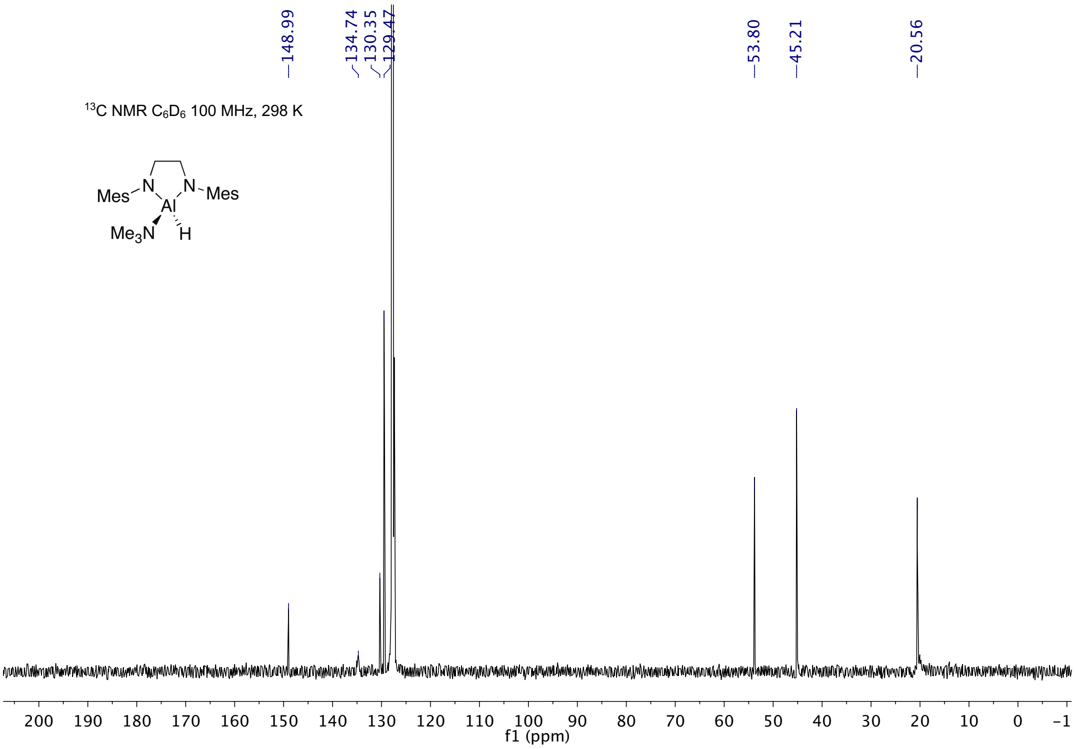
148.99
134.74
130.35
129.47
53.80
45.21
20.56
^{13}C NMR C_6D_6 100 MHz, 298 K
Mes
N
N
Mes
Al
Me_3N
H
200
190
180
170
160
150
140
130
120
110
100
90
80
70
60
50
40
30
20
10
0
–1
f1 (ppm)

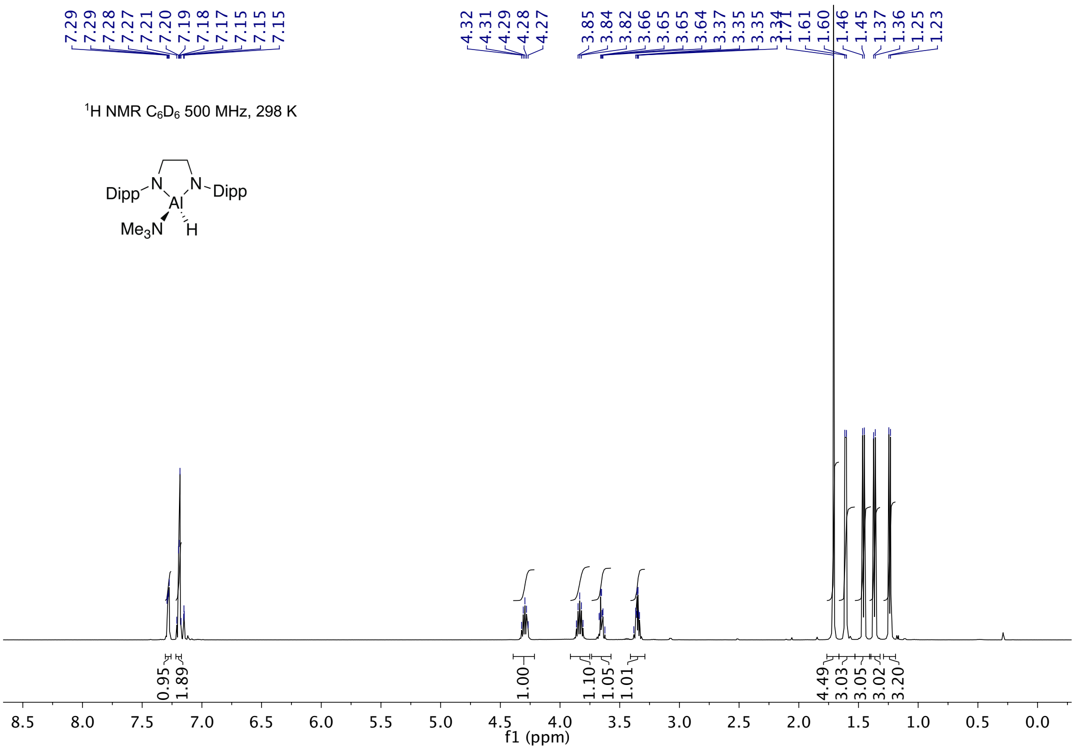
7.29
7.29
7.28
7.27
7.21
7.20
7.19
7.18
7.17
7.15
7.15
7.15
4.32
4.31
4.29
4.28
4.27
3.85
3.84
3.82
3.66
3.65
3.65
3.64
3.37
3.35
3.35
3.34
1.71
1.61
1.60
1.46
1.45
1.37
1.36
1.25
1.23
^{1}H NMR C_6D_6 500 MHz, 298 K
Dipp
N
N
Dipp
Al
Me_3N
H
0.95
1.89
1.00
1.10
1.05
1.01
4.49
3.03
3.05
3.02
3.20
8.5
8.0
7.5
7.0
6.5
6.0
5.5
5.0
4.5
4.0
3.5
3.0
2.5
2.0
1.5
1.0
0.5
0.0
f1 (ppm)

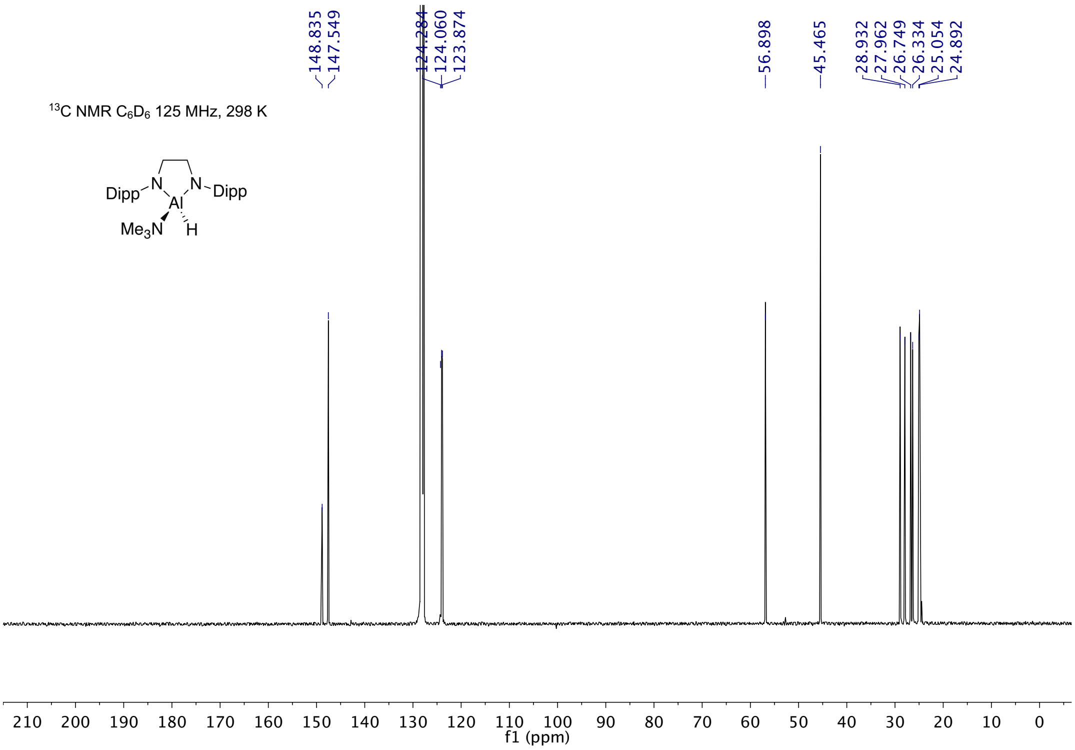
148.835
147.549
124.284
124.060
123.874
56.898
45.465
28.932
27.962
26.749
26.334
25.054
24.892
^{13}C NMR C_6D_6 125 MHz, 298 K
Dipp
N
N
Dipp
Al
Me_3N
H
210
200
190
180
170
160
150
140
130
120
110
100
90
80
70
60
50
40
30
20
10
0
f1 (ppm)

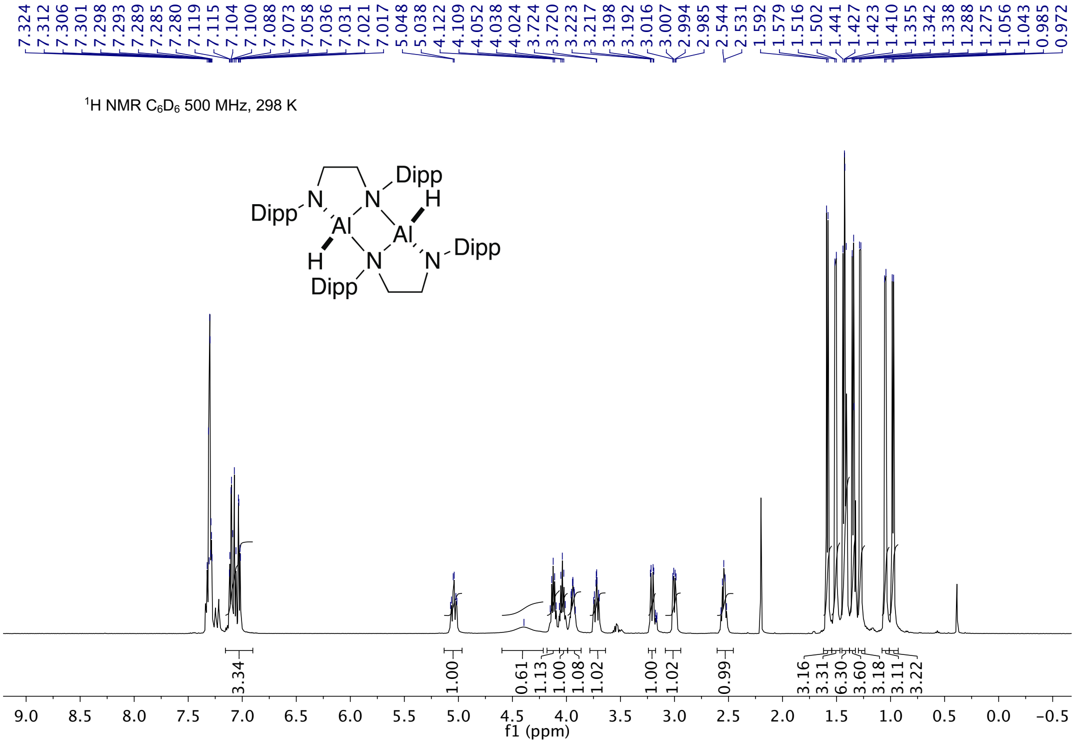
7.324 7.312 7.306 7.301 7.298 7.293 7.289 7.285 7.280 7.119 7.115 7.104 7.100 7.088 7.073 7.058 7.036 7.031 7.021 7.017 5.048 5.038 4.122 4.109 4.052 4.038 4.024 3.724 3.720 3.223 3.217 3.198 3.192 3.016 3.007 2.994 2.985 2.544 2.531 1.592 1.579 1.516 1.502 1.441 1.427 1.423 1.410 1.355 1.342 1.338 1.288 1.275 1.056 1.043 0.985 0.972
^{1}H NMR C_6D_6 500 MHz, 298 K
Dipp
N
N
H
Al
Al
N
N
Dipp
Dipp
H
Dipp
3.34
1.00
0.61
1.13
1.00
1.08
1.02
1.00
1.02
0.99
3.16
3.31
6.30
3.60
3.18
3.11
3.22
9.0 8.5 8.0 7.5 7.0 6.5 6.0 5.5 5.0 4.5 4.0 3.5 3.0 2.5 2.0 1.5 1.0 0.5 0.0 −0.5
f1 (ppm)

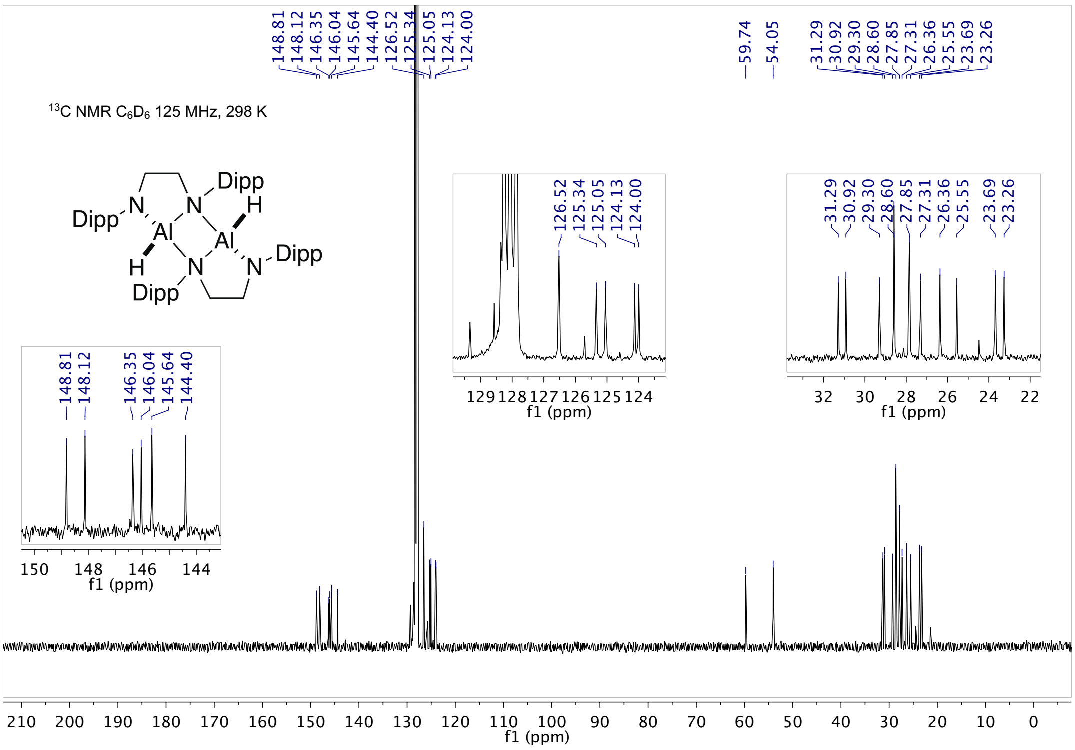
148.81 148.12 146.35 146.04 145.64 144.40 126.52 125.34 125.05 124.13 124.00
59.74
54.05
31.29 30.92 29.30 28.60 27.85 27.31 26.36 25.55 23.69 23.26
^{13}C NMR C_6D_6 125 MHz, 298 K
Dipp
N
N
H
Al
Al
N
N
Dipp
Dipp
H
Dipp
148.81 148.12 146.35 146.04 145.64 144.40
150 148 146 144
f1 (ppm)
126.52 125.34 125.05 124.13 124.00
129 128 127 126 125 124
f1 (ppm)
31.29 30.92 29.30 28.60 27.85 27.31 26.36 25.55 23.69 23.26
32 30 28 26 24 22
f1 (ppm)
210 200 190 180 170 160 150 140 130 120 110 100 90 80 70 60 50 40 30 20 10 0
f1 (ppm)

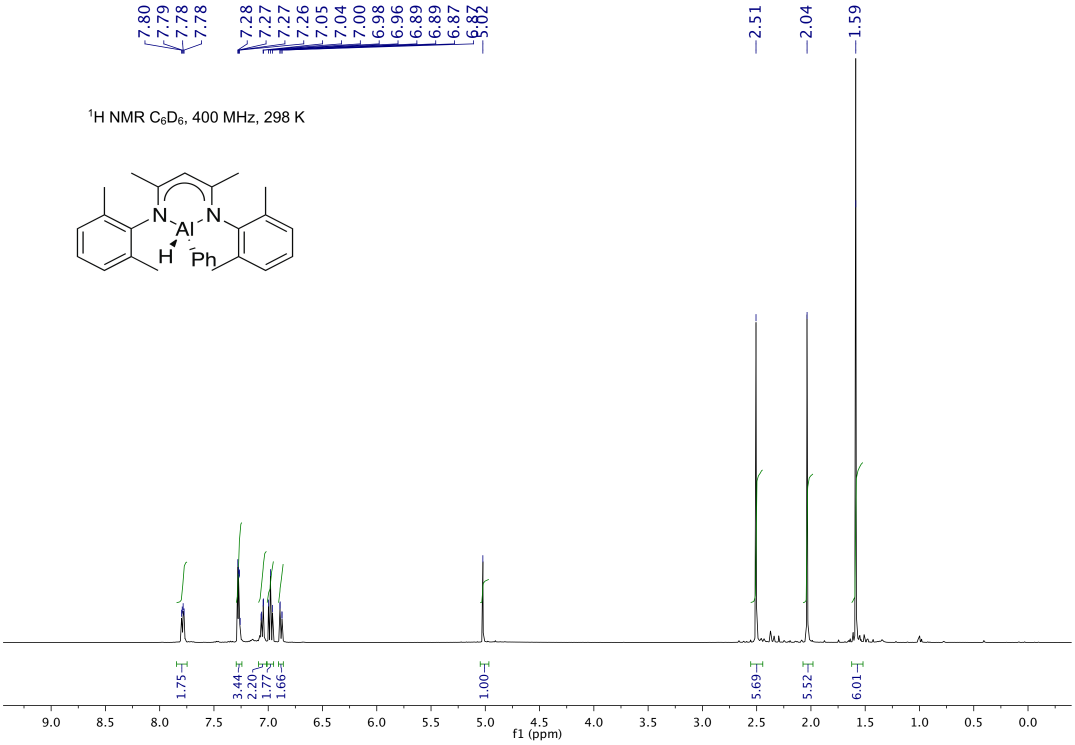
7.80
7.79
7.78
7.78
7.28
7.27
7.27
7.26
7.05
7.04
7.00
6.98
6.96
6.89
6.89
6.87
6.87
5.02
2.51
2.04
1.59
¹H NMR C₆D₆, 400 MHz, 298 K
N
Al
N
H
Ph
1.75
3.44
2.20
1.77
1.66
1.00
5.69
5.52
6.01
9.0
8.5
8.0
7.5
7.0
6.5
6.0
5.5
5.0
4.5
4.0
3.5
3.0
2.5
2.0
1.5
1.0
0.5
0.0
f1 (ppm)

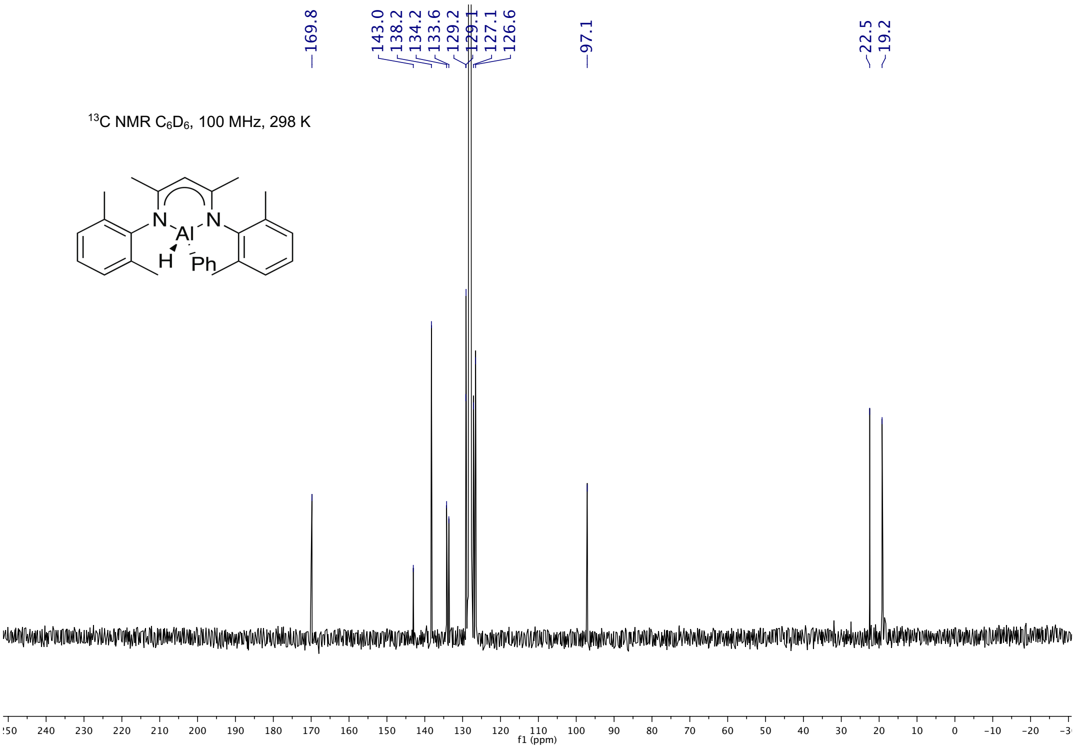
169.8
143.0
138.2
134.2
133.6
129.2
129.1
127.1
126.6
97.1
22.5
19.2
¹³C NMR C₆D₆, 100 MHz, 298 K
N
Al
N
H
Ph
250
240
230
220
210
200
190
180
170
160
150
140
130
120
110
100
90
80
70
60
50
40
30
20
10
0
-10
-20
-30
f1 (ppm)